(26) E. A. Collins, J. Bares, and F. W. Billmeyer, "Experiments in Polymer Science", Wiley, New York, 1973.
(27) F. Rodriguez, "Principles of Polymer Systems", 2nd ed., McGraw-Hill, New York, 1982.
(28) S. C. Misra, J. A. Manson, and L. H. Sperling, *ACS Symp. Ser.*, **No. 114**, 157 (1979).
(29) S. S. Labana, S. Newman, and A. J. Chompff, in "Polymer Networks", A. J. Chompff and S. Newman, Eds., Plenum Press, New York, 1971, p 453.
(30) E. G. Bobalek, E. R. Moore, S. S. Levy, and C. C. Lee, *J. Appl. Polym. Sci.*, **8**, 625 (1964).
(31) K. Dusek, in "Developments in Polymerizations", Vol. 3, R. N. Haward, Ed., Applied Science Publishers, London, 1982.
(32) K. Dusek, J. Plestil, F. Lednicky, and S. Lunick, *Polymer*, **19**, 393 (1978).
(33) K. Dusek and M. Ilavsky, *Polym. Eng. Sci.*, **19**, 393 (1978).
(34) D. H. Solomon, B. C. Loft, and J. D. Swift, *J. Appl. Polym. Sci.*, **11**, 1593 (1967).
(35) L. Gallacher and F. A. Bettelheim, *J. Polym. Sci.*, **58**, 697 (1962).
(36) K. Dusek, in "Polymer Networks", A. J. Chompff and S. Newman, Eds., Plenum Press, New York, 1971, p 245.
(37) W. Klonowski, *Rheol. Acta*, **18**, 673 (1979).
(38) J. Guillot, *Makromol. Chem.*, **183**, 619 (1982).
(39) H. M. J. Boots and R. B. Pandey, *Polym. Bull.*, **11**, 415 (1984).
(40) M. Barthelin, G. Boissier, and J. Dubois, *Makromol. Chem.*, **182**, 2075 (1981).
(41) P. W. Kwant, *J. Polym. Sci., Polym. Chem. Ed.*, **17**, 1331 (1979).
(42) R. H. Wiley and E. E. Sale, *J. Polym. Sci.*, **42**, 491 (1960).
(43) R. H. Wiley, S. Rao, J. Jin, and K. S. Kim, *J. Macromol. Sci., Chem.*, **A4**, 1453 (1970).
(44) G. Schwachula, *J. Polym. Sci., Polym. Symp.*, **No. 53**, 107 (1975).
(45) B. T. Storey, *J. Polym. Sci., Part A*, **3**, 265 (1965).
(46) J. Malinsky, J. Klaban, and K. Dusek, *J. Macromol. Sci., Chem.*, **A5**, 1071 (1971).
(47) P. J. Flory, "Principles of Polymer Chemistry", Cornell University Press, Ithaca, NY, 1953.
(48) W. H. Stockmayer, *J. Chem. Phys.*, **12**, 125 (1944).
(49) Z. Rigbi, in "Polymer Networks", A. J. Chompff and S. Newman, Eds., Plenum Press, New York, 1971, p 245.
(50) L. H. Sperling, "Interpentrating Polymer Networks and Related Materials", Plenum Press, New York, 1981, p 49.
(51) D. L. Siegfried, D. A. Thomas, and L. H. Sperling, *Macromolecules*, **12**, 586 (1979).
(52) Note that the use of "excluded volume" in this context—unswellable or inaccessible polymer regions due to cross-link density variations—should not be confused with the definition used in many theories in which "excluded volume" is defined as the fact that a given polymer molecule excludes others or itself from occupying its immediate place in space,[47] although the concepts are similar. In this case "excluded volume" refers to supermolecular regions.

Chain Conformation in Medium and High Ester Content Polyether–Polyester Block Copolymers: A Small-Angle Neutron Scattering Study

John A. Miller, J. Michael McKenna,† Gerfried Pruckmayr,† J. Ernest Epperson,‡ and Stuart L. Cooper*

Department of Chemical Engineering, University of Wisconsin, Madison, Wisconsin 53706.
Received December 11, 1984

ABSTRACT: The conformation of the polyether soft segment, the polyester hard segment, and the entire chain was measured as a function of temperature in two series of polyether–polyester multiblock copolymers using small-angle neutron scattering. At room temperature, the average soft segment was found to be in a slightly expanded random coil conformation, although some of the segments are probably extended. The measured soft-segment radius of gyration decreased somewhat as the sample was heated. This behavior was attributed to the presence of fewer taut soft segments due to the relaxation of stresses in the material as the chains become more mobile above the glass transition temperature of the hard segments. The crystallized hard segments exhibited a chain-folded structure at room temperature. The measured fold length was 3–4 hard-segment units long. The hard-segment radius of gyration increased substantially as the temperature was increased. This is attributed to the unfolding of some segments by a melting and recrystallization of the highly folded segments and to new hard segments crystallizing out of the amorphous phase into an extended crystalline conformation. The radius of gyration of the whole chain decreased as the temperature was increased between 25 and 150 °C. The reason for this is unclear, although it may be due to the relaxation of the stresses introduced into the system by molding the sample below the hard-segment crystalline melting temperature. Above 160 °C, the crystallization of new hard-segment material becomes an important process, along with lamellar thickening. These processes cause the radius of gyration of the whole chain to increase.

Introduction

Polyether–polyester block copolymers are segmented thermoplastic elastomers that exhibit excellent physical properties and chemical resistance. They are marketed by E. I. du Pont de Nemours and Co. under the trade name of Hytrel. Polyether–polyesters exhibit a two-phase microstructure, which is responsible for their superior mechanical characteristics. The two phases present in Hytrel systems are an amorphous phase and a crystalline or semicrystalline phase. The amorphous phase, also called the soft phase, consists of a mixture of polyether and polyester segments, which are also known as the soft and hard segments, respectively. The crystalline phase consists almost exclusively of crystallized polyester segments. The service temperature of the material lies between the glass transition temperature of the soft phase and the crystalline melting temperature of the hard phase. The microstructure of these materials at intermediate polyester compositions features a soft, rubbery matrix filled with a hard, reinforcing phase that acts as a physical cross-linker. The major driving force for phase separation in the polyether–polyester systems is the crystallization of the hard polyester segments. Any contribution to the driving force due to the incompatibility of the ester and ether segments is smaller in magnitude, unlike the situation in polyurethane block copolymers, where the driving force is usually dominated by intersegmental repulsion. Chemical structure and processing conditions are also known to

†E. I. du Pont de Nemours and Co., Wilmington, DE 19898.
‡Argonne National Laboratory, Argonne, IL 60439.

0024-9297/85/2218-1727$01.50/0

affect the degree of phase separation in polyether–polyesters.

A number of recent studies have been made on the morphology of polyether–polyester block polymers[1-9] and related monodisperse model polyether–polyester compounds.[10] Polyether–polyesters with a hard-segment content above 24% are found to have a two-phase microstructure[7] due to the presence of hard-segment subsequences with more than two repeat units, which tend to segregate much more readily than do shorter hard segments. This is consistent with the results of Miller et al.,[11] who in a study of a series of polyether–polyurethanes found that single repeat unit hard segments are more soluble in the soft phase than are longer hard segments. The polyether–polyesters have been shown to possess a lamellar or pseudolamellar microstructure. The lamellar hard domains are also surprisingly regular in size and shape, similar to the structure in semicrystalline homopolymers.[7] This regularity in lamellar thickness has been taken as evidence for folding of the polyester segments, since there is a relatively broad distribution of hard-segment lengths. The interface between the two phases has been shown to be fairly sharp[8,9] using small-angle X-ray scattering (SAXS). In addition, a distinct spherulitic macrostructure is often observed.

Small-angle neutron scattering (SANS) has recently been used to examine chain conformation in bulk polymer samples. The great power of this technique comes from the difference in scattering lengths between the two common hydrogen isotopes. By substituting deuterium for hydrogen in a polymer chain, one can provide a contrast mechanism for the SANS experiments without altering the chemistry of the system being investigated. An analogous labeling experiment for X-ray scattering invariably changes the chemical interactions present in the system. The first use of SANS to study the chain conformation in polymer materials was by Ballard et al.,[12] who found that polystyrene chains in a bulk, amorphous sample were in the random flight or Gaussian conformation, confirming the hypothesis of Flory.[13] Subsequent studies on other amorphous polymers yielded the same conclusion and are reviewed by Higgins and Stein[14] and Richards.[15]

Small-angle neutron scattering more recently has been applied to phase-separated block copolymer systems. The chain conformation of the individual blocks can be obtained by two different methods. The first involves utilization of polymer samples with a well-defined microstructure. Hadziioannou et al.[16] investigated the conformation of the styrene block in a very regular lamellar styrene/isoprene block copolymer. The styrene phase contained both purely deuterated and purely protonated chains. When the plane of the lamellar surface was aligned perpendicular to the incident neutron beam, the interphase scattering due to interference between the lamellae was nearly eliminated. This left only the chain scattering from the labeled and unlabeled styrene chains, from which the styrene chain conformation was obtained. These researchers found that the styrene chains were in an extended conformation relative to the bulk polystyrene homopolymer in the direction perpendicular to the lamellar surface.

The second method for extracting the single-chain scattering function for a single block within one phase of a two-phase block copolymer makes use of the scattering theory developed independently by Koberstein[17] and Jahshan and Summerfield.[18,19] The basic principle of this theory is that the single-chain scattering function can be obtained by a weighted subtraction of the scattering curves

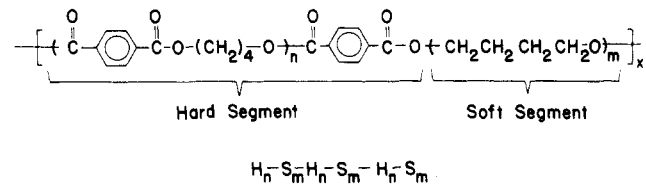

Figure 1. Repeat-unit structure of the polyether–polyesters.

Table I
Mole Ratios of Reactants Used in the Syntheses

sample	DMT	d-DMT	BD	d-BD	PTMO	d-PTMO
5-1	5	0	4	0	1	0
5-2	5	0	4	0	0.2762	0.7238
5-3	5	0	4	0	0.6834	0.3166
5-4	0	5	0	4	1	0
5-5	0	5	0	4	0	1
10-1	10	0	9	0	1	0
10-2	10	0	9	0	0.2816	0.7184
10-3	10	0	9	0	0.6930	0.3070
10-4	0	10	0	9	1	0
10-5	0	10	0	9	0	1

of two samples. The first sample consists entirely of undeuterated chains. The second sample features one of the segment types having both protonated and deuterated chains. Bates et al.[20] applied this method to a diblock copolymer of styrene and butadiene, with the butadiene chains being the labeled species. The morphology exhibited by this system consisted of spherical butadiene domains within a styrene matrix. The butadiene chain conformation was found to be the same as for bulk butadiene homopolymer. Miller et al.[21] investigated the conformation of the soft segment in a polyether–polyurethane multiblock copolymer by the same method. In that study, a series of samples that were nearly morphologically identical were prepared with different levels of deuteration of the poly(tetramethylene oxide) (PTMO) soft segment. As the degree of deuteration rose, the contrast between the hard and soft phase decreased. The portion of the coherent scattering that was due to the chain scattering from the soft segments therefore increased, while the interphase scattering decreased. The authors found that the polyether chain conformation was somewhat extended in this block copolymer relative to the conformation of the bulk oligomeric PTMO.

The objective of the present investigation was to extend the application of SANS to polyether–polyester multiblock copolymers in order to obtain the conformation of the polyether segment, the hard polyester segment, and the overall polymer chain. It was also desirable to obtain information regarding the change in segment and chain conformation as a function of temperature in order to better understand the processes involved in phase separation and annealing.

Experimental Section

The polyether–polyester block copolymers were synthesized by a melt transesterification reaction involving dimethyl terephthalate (DMT), butanediol (BD), and a poly(tetramethylene oxide) (PTMO) oligomer, as described by Witsiepe.[22] The materials synthesized are listed in Table I. The polymer repeat structure is shown in Figure 1. The deuterated DMT and the deuterated butanediol, both with an isotopic purity of 99.3%, were obtained from Merck, Sharp, and Dohme, Inc. and used as received. The deuterated PTMO was synthesized by a ring-opening polymerization reaction. The d-PTMO had a number-average molecular weight of 945. The protonated PTMO used was Du Pont Teracol 1000, a commercial material with a number-average molecular weight of 1000. The samples used for the scattering

Table II
Composition of Scattering Samples Based on Moles of Polyester Segments and Table I

sample	$n-1$	$n-2$	$n-3$	$n-4$	$n-5$
5-SS	0	0	1	0	0
5-HS	0	0.7066	0	0.2934	0
5-WC	0.0576	0	0	0	0.9424
10-SS	0	0	1	0	0
10-HS	0	0.7069	0	0.2931	0
10-WC	0.0243	0	0	0	0.9757

experiments were prepared by blending the materials synthesized in Table I according to the ratios given in Table II. The blending was done by dissolving the materials in 1,1,2-trichloroethane at 50 °C, followed by drying under vacuum at 40 °C for 1 week. The samples were then molded at 200 °C for 5 min at 20 MPa and cooled to room temperature over a time span of 5 min. The samples were stored in a desiccator until needed for the scattering experiments.

The numeric portion of the sample description indicates the number of DMT units in the average hard segment. The letter description indicates the particular segment conformation being investigated with that sample. -SS implies that the sample is being used to find the soft-segment conformation, while -HS and -WC mean that these samples are being used to measure the hard-segment and whole-chain conformations. Thus, 10-HS is a sample with an average hard-segment length of 10 tetramethylene terephthalate (TMT) units and is used to determine the hard-segment conformation.

The small-angle neutron scattering data were obtained on the intense pulsed neutron source (IPNS) at Argonne National Laboratory on the small-angle diffractometer (SAD) instrument. This facility has been described in detail elsewhere.[24] The range of the magnitude of the scattering vector q, where $q = (4\pi/\lambda) \sin \theta$, λ is the incident neutron wavelength, and θ is the scattering angle, is from 0.008 to 0.350 Å^{-1}. The other operating conditions for this experiment were a resolution of 0.004 Å^{-1} and a flux at the sample of $\sim 4 \times 10^4$ neutrons/(s cm^2). The samples were held at a fixed temperature inside a helium-purged vacuum furnace while the scattering data were being gathered. Data were collected for about 4 h at each temperature level, giving a total count of $\sim$200 000 neutrons.

Theory

The neutron scattering from a two-phase system where one of the phases consists of a blend of labeled and unlabeled chains has been described by Koberstein.[13]

$$(R_L(q) - R_{inc,L}) - \left[\frac{\beta_A - x\beta_{BD} - (1-x)\beta_{BH}}{\beta_A - \beta_{BH}}\right]^2 (R_U(q) - R_{inc,U}) = \frac{4\pi}{V_s}(b_{BD} - b_{BH})^2 N_{BT} Z_B^2 x(1-x) P_B(q) \quad (1)$$

In this expression, $R_L(q)$ and $R_U(q)$ are the total Rayleigh factors for a partially labeled sample and a completely unlabeled sample and $R_{inc,L}$ and $R_{inc,U}$ are the incoherent background scattering terms for these samples. β_A is the coherent scattering length density of pure A segments, β_{BH} and β_{BD} are the coherent scattering length densities for pure protonated B segments and pure deuterated B segments, and x is the fraction of the B chains that are deuterated. V_s is the irradiated sample volume, b_{BH} and b_{BD} are the monomeric coherent scattering lengths for the protonated and deuterated B monomers, N_{BT} is the total number of B chains present in the scattering volume, and Z_B is the average degree of polymerization of the B segments. $P_B(q)$ is the single-chain scattering function, also known as the structure or form factor for the B segments or as the intramolecular interference function. $P_B(q)$ contains the information on the chain conformation available from neutron scattering.

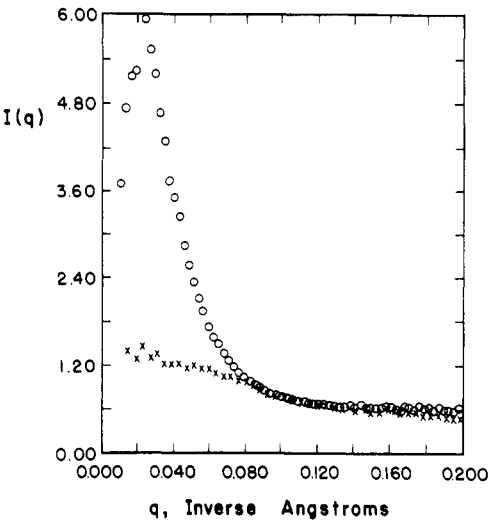

Figure 2. SANS data for the 5/4/1 composition polyether–polyesters. The (×) represents the phase contrast matched sample, 5-SS, while the (○) denotes the scattering from a sample with no deuteriolabeling. The scattering in this case is due only the the two-phase microstructure. The data shown are at room temperature.

Equation 1 states that $P_B(q)$ can be obtained by the subtraction of the scattering by an unlabeled sample from that of a labeled sample. The subtraction is weighted by the term in brackets that appears on the left-hand side of eq 1. For one particular value of x, the degree of deuteration of the B chains, this weighting factor is zero. This condition is known as the phase contrast matched condition.[21] It is described by

$$\beta_A - x\beta_{BD} - (1-x)\beta_{BH} = 0 \quad (2)$$

When this condition is true for the labeled sample, there is no need to measure the scattering from an unlabeled sample. This makes the results of the scattering experiment easier to interpret and more reliable, as has been shown by Miller et al.[21] There is no need to match the morphology of two samples exactly, which is a requirement for using eq 1. This is often difficult for multiblock copolymer systems. Figure 2 shows scattering data from a labeled, phase contrast matched system and from an unlabeled sample of the same chemical composition. The samples shown are the 5-SS sample and an unlabeled sample with a 5/4/1 molar composition. The most prominent feature in this figure is the absence of peak due to interphase scattering in the phase contrast matched sample. The intensity of the maximum due to interphase scattering in the unlabeled curve is substantially larger than the magnitude of the intrachain scattering from the 5-SS sample.

The phase contrast matching criterion can be extended to include partial labeling of both phases. The restriction here is that the coherent scattering length densities of both pure phases be the same. The phase contrast matching requirement is met by a linear function of the degree of deuteration of the soft segments and of the hard segments.

$$(y\beta_{AD} + (1-y)\beta_{AH}) - (x\beta_{BD} + (1-x)\beta_{BH}) = 0 \quad (3)$$

In this expression x and y are the fractional deuteration levels of the soft and hard segments, respectively. This expression implies that an increase in the hard-phase coherent scattering length density caused by labeling the hard segments can be offset by deuterating the soft segments to a greater extent.

One concern when using a phase contrast matched sample is that the degree of deuteration of the soft phase

Table III
Distribution of Polyester Sequence Lengths for 5- and 10-Series Materials

DMT units	5-series	10-series	DMT units	5-series	10-series
1	0.2000	0.1000	14	0.0109	0.0254
2	0.1600	0.0900	15	0.0087	0.0228
3	0.1280	0.0810	16	0.0070	0.0205
4	0.1024	0.0729	17	0.0056	0.0185
5	0.0819	0.0656	18	0.0045	0.0166
6	0.0655	0.0590	19	0.0036	0.0150
7	0.0524	0.0531	20	0.0028	0.0135
8	0.0419	0.0478	21	0.0023	0.0121
9	0.0335	0.0430	22	0.0018	0.0109
10	0.0268	0.0387	23	0.0014	0.0098
11	0.0214	0.0348	24	0.0011	0.0088
12	0.0171	0.0313	25	0.0009	0.0079
13	0.0137	0.0282			

will be quite high. This may result in a substantial effect on the scattering due to interchain interference. However, Akcasu et al.[25] and Wignall et al.[26] have shown that the level of deuteration has little or no effect on the radius of gyration measured by SANS. Having a substantial fraction of the soft-segment chains being labeled also causes concern over the correlation of the individual labeled segments. If the correlation is strong, chain sub-sequences of the type S–H–S, where S and H refer to the soft and hard segments, will contribute substantially to the scattering when only single S unit scattering is desirable.

For S–H–S sub-sequences to contribute to the scattering as an entity larger than a single S unit, both soft segments in the sub-sequence must be deuterated. If one S is protonated and one is deuterated, only scattering from a single S unit will occur. Roughly 9% of the sub-sequences of the S–H–S type will have both soft segments deuterated in the -SS samples. The scattering intensity from the S–H–S sequences when both soft segments are deuterated is proportional to the product of the number of S_d–H–S_d sequences and the number of S_h–H–S_h sequences, where d and h refer to the deuterated and protonated soft segments. For the -SS samples, this product is around 4–5% of the coherent scattering.

Not all of the S_d–H–S_d sequences will contribute to the scattering as a species larger than a single S unit. For example, when the intervening hard segment is part of a hard-phase crystallite, the soft-segment chains will be independent. Lilaonitkul and Cooper[3] and Vallance et al.[4] report that roughly 50% of the polyester segments are located within hard crystalline domains for materials with about the same chemical compositions as those studied in this investigation. The presence of a long polyester sequence between the soft segments will also cause the soft segments to be relatively independent. Peebles[27,28] has derived the equations governing the sequence length distributions in multiblock copolymers synthesized by either a one-step or two-step polymerization. The polyester sequence length distributions for the first 25 TMT units have been calculated by using Peebles' equations and are listed in Table III. A hard segment that is n TMT units long contains $(n - 1)$ butanediol monomers. The smallest hard segment is therefore a single DMT unit. When all of the above factors are taken into consideration, the overall contribution to the scattering from deuterated S–H–S sub-sequences is quite small, on the order of 1–2% of the total scattering. This is within the error of the experiment, thus this contribution can safely be ignored.

For the phase contrast matched -SS samples we can describe the coherent the scattering by

$$R_{SS}(q) = (4\pi/V_s)(b_{SD} - b_{SH})^2 N_S Z_S^2 x_{SS}(1 - x_{SS}) P_S(q) \quad (4)$$

Similar expressions can be written for the -HS samples and the -WC samples.

$$R_{HS}(q) = \frac{4\pi}{V_s}(b_{SD} - b_{SH})^2 N_S Z_S^2 x_{HS}(1 - x_{HS}) P_S(q) + \frac{4\pi}{V_s}(b_{HD} - b_{HH})^2 N_H Z_H^2 y_{HS}(1 - y_{HS}) P_H(q) \quad (5)$$

$$R_{WC}(q) = \frac{4\pi}{V_s}(b_{SD} - b_{SH})^2 N_S Z_S^2 x_{WC}(1 - x_{WC}) P_S(q) + \frac{4\pi}{V_s}(b_{HD} - b_{HH})^2 N_H Z_H^2 y_{WC}(1 - y_{WC}) P_H(q) + \frac{4\pi}{V_s}(b_{WD} - b_{WH})^2 N_W Z_W^2 z_{WC}(1 - z_{WC}) P_W(q) \quad (6)$$

In these expressions, $R_{SS}(q)$, $R_{HS}(q)$, and $R_{WC}(q)$ refer to the coherent scattering from the specified samples. The subscripts SS, HS, and WC refer to properties of the specific samples. As before, x and y are the fraction of deuteration of the soft and hard segments, while z is the fraction of whole chains that are deuterated. $P_S(q)$, $P_H(q)$, and $P_W(q)$ are the single-chain scattering functions for the soft and hard segments and the whole chain.

To this point we have been dealing with two-phase systems that possess pure phases. The effect of phase mixing, i.e., the presence of hard segments in the soft phase and vice versa, must be considered. It can be shown that phase mixing has no effect on the phase contrast matched condition of eq 3. This is not surprising, since if the pure phases have the same contrast, then a mixture of the pure phases would also be expected to have the same contrast. One can then calculate the degree of deuteration that will produce zero interphase scattering provided that the pure-phase densities are known with reasonable accuracy. Knowledge of the mixed-phase densities and compositions is not necessary. Also, changes in the degree of phase separation, such as may occur upon annealing, will not change the phase contrast matched properties of the sample.

Although the phase contrast matching criterion is independent of the degree of phase mixing in a sample, one must consider the effect of phase mixing on the chain scattering from the sample. Ideally the SANS experiments will product intrachain scattering due to the contrast between isotopically different segments and not between chemically different segments. The amorphous soft phase in this experiment is composed of a blend of protonated hard segments and deuterated and protonated soft segments. Hadziioannou et al.[29] give the scattering equation from a two-component single-phase blend where one of the components is partially labeled, such as the soft phase in this experiment. This expression is

$$R_L(q) = \frac{4\pi}{V_s}(b_{BD} - b_{BH})^2 N_{BT} Z_B^2 x(1 - x) P_B(q) + \frac{4\pi}{V_s}\left[x b_{BD} + (1 - x) b_{BH} - b_A\left(\frac{V_B}{V_A}\right)\right]^2 N_{BT} Z_B^2 (P_B(q) + N_{BT} Q_{BB}(q)) \quad (7)$$

where V_A and V_B are the molar volumes of the repeat units for A and B. $Q_{BB}(q)$ is the intermolecular interference function. The prefactor in brackets for the second part of the right-hand side of eq 7 is zero whenever the phase contrast matched condition applies. Since this prefactor multiplies the only intermolecular interference term, when the sample is phase contrast matched, the only coherent scattering that occurs is due to the labeled and unlabeled B segments. Generalizing this to the case where both the soft segments and the hard segments are a blend of deu-

terated and protonated species, in a phase contrast matched material, the only coherent scattering that occurs is due to correlations between labeled and unlabeled segments of the same type. There is no contribution due to interphase scattering or due to correlations between the different segment types.

Once the chain scattering has been obtained by a SANS experiment, the components of the single-chain scattering must be separated. In the -SS sample, the chain scattering is due only to the soft segments and no separation is necessary. For the -HS samples, both soft-segment and hard-segment single-chain scattering are present. Since the soft-segment single-chain scattering is a known quantity from the results of the -SS experiment and the sample composition, one can easily separate the hard- and soft-segment scattering contributions by a weighted subtraction using eq 4 and 5. Similarly, in the -WC experiment, weighted subtractions of both the hard- and soft-segment single-chain scattering using eq 4–6 yield the single-chain scattering from the total chain.

The single-chain scattering function can be modeled by a number of different particle shapes. For particles where the actual shape is not known, the approximation of Guinier[30] can be applied.

$$\lim_{q\to 0} I(q) = Ke^{-q^2R_g^2/3} \tag{8}$$

In this expression, R_g is the radius of gyration of the particle and K is a proportionality constant. This model is used at low values of q, which limits its usefulness. A number of researchers have applied Guinier's law beyond values of $qR_g = 1$ due to the limitations of SANS instruments at low angles; however, strictly speaking, this is not correct. A better approach is to use all of the available scattering data by fitting a model for the chain conformation to the data. By this method, a better interpretation of the data should be possible, if only because more of the scattering data is used for the analysis. It is important to remember in this approach that the results are dependent on the particular model chosen. Generally the trends found by such a model-fitting procedure are correct, although absolute numbers obtained may be in error if an improper model is selected.

For amorphous polymer chains, the chain geometry can be modeled as a random coil. The structure factor for a random coil is described by the Debye function

$$F(q) = \frac{2}{t^2}(e^{-t} + t - 1) \tag{9}$$

where $t = q^2R_g^2$ and R_g is the radius of gyration of the coil. This model has been found to be an excellent choice for amorphous bulk homopolymers.[10,11] The crystalline hard-segment chains are not likely to be in a random coil conformation. The single-chain scattering observed for the hard segments is an average of the contributions from the hard segments that are in the amorphous soft phase and the hard segments that are crystallized in the hard phase. Choosing a model that accurately represents both the crystallized and the amorphous hard-segment conformations is not possible. Some compromise must be made. Two models in addition to the random coil were used to model the average hard-segment conformation: an infinitesimally thin rod and a cylinder. A cylindrical model was used along with the random coil to model the overall chain conformation. The form factor for a cylinder is given by

$$F(q) = \int_0^{\pi/2} \frac{\sin(0.5qL\cos\theta)}{(0.5qL\cos\theta)^2} \frac{4J_1(qR\cos\theta)}{(qR\cos\theta)^2} d\theta \tag{10}$$

where L is the length of the cylinder, R is the radius of the cylinder, and J_1 is a first-order Bessel function of the first kind. The form factor for an infinitesimally thin rod is given by

$$F(q) = \frac{\mathrm{Si}(qL)}{qL} - \frac{4\sin^2(0.5qL)}{(qL)^2} \tag{11}$$

where L is the length of the rod and Si (x) is defined as

$$\mathrm{Si}(x) = \int_0^x \frac{\sin(y)}{y} dy \tag{12}$$

The corresponding radii of gyration for these two models are

$$R_g^2 = L^2/12 + R^2/2 \quad \text{(cylinder)} \tag{13a}$$

$$R_g^2 = L^2/12 \quad \text{(rod)} \tag{13b}$$

The structure factors given in eq 9–12 are part of the generalized model used to fit the scattering data. The general model is

$$I(q) = AF(q) + I_{inc} \tag{14}$$

where A is a proportionality constant and I_{inc} is the incoherent scattering, which is independent of q.[17] I_{inc} was found to increase gradually with temperature, in agreement with the prediction of Maconnachie.[42] Equation 14 was fit to the single-chain scattering data using a least-squares nonlinear regression routine that generates best fit parameters as well as error estimates. For the Debye model and the rod model, the radius gyration was fit along with A and I_{inc}. For the cylinder model, an additional parameter, the aspect ratio of the cylinder, was fit.

The values obtained for the radius of gyration of a segment through the fitting of eq 14 are z-average values. To correct for the polydispersity of the samples, the distribution of segment lengths must be known along with knowledge of how the radius of gyration changes as a function of the molecular weight. The applicable polydispersity equations are

$$\frac{\langle R_g^2\rangle_z}{\langle R_g^2\rangle_w} = \frac{\sum_{i=1}^{\infty} N_iM_i^2R^2(i)}{\sum_{i=1}^{\infty} N_iM_i^2} \frac{\sum_{i=1}^{\infty} N_iM_i}{\sum_{i=1}^{\infty} N_iM_iR^2(i)} \tag{15a}$$

$$\frac{\langle R_g^2\rangle_z}{\langle R_g^2\rangle_n} = \frac{\sum_{i=1}^{\infty} N_iM_i^2R^2(i)}{\sum_{i=1}^{\infty} N_iM_i^2} \frac{\sum_{i=1}^{\infty} N_i}{\sum_{i=1}^{\infty} N_iR^2(i)} \tag{15b}$$

where the n, w, and z subscripts refer to the average being taken, N_i is the number of species that are i monomer units long, M_i is the molecular weight of a segment that is i monomers long, and $R(i)$ is the radius of gyration of a segment that is i monomers long. For the hard segment, i is the number of TMT units. For the soft segment, i is the number of tetrahydrofuran monomers in the PTMO oligomer. Values for N_i have been calculated for the hard segments and are listed in Table III. The distribution of the soft-segment lengths was determined previously by high-performance liquid chromatography (HPLC).[23] The values for M_i are easily found from the chemical structure of the segments.

The dependence of the radius of gyration on the degree of polymerization is not as easy to determine. In general, $R(i)$ can be written as

$$R(i) = KM^{\alpha} \quad (16)$$

where K is a proportionality constant. Establishing a value for α is important in order to accurately determine the polydispersity correction. For a random coil, α has a value of $^1/_2$. For a cylinder that expands equally in all directions as the molecular weight increases, α is $^1/_3$. For an infinitesimally thin rod, α equals 1. The lamellae in polyether–polyester materials have been found to possess a fairly uniform thickness regardless of the hard-segment length.[7] Thus as the molecular weight of the hard segments increases, the lamellae only increase in size in a lateral direction. In this case, the radius of gyration of the hard domain increases as the one-half power of M. The actual value of α is dependent upon many factors. For the soft segment, the value of α is $^1/_2$ since it is likely to be near a random coil conformation. Deviations in α for low molecular weight species have a very small effect on the polydispersity correction, since the random coil approximation is valid for bulk PTMO down to around a molecular weight of 400–500.[43] As a first approximation, α is taken to be $^1/_2$ for the hard segment and for the whole chain.

The sample compositions were selected by using three basic principles. First, the samples used for scattering must be phase contrast matched. This maximizes the signal-to-noise factor in the experiment and eliminates the need for a subtraction of the scattering from an unlabeled sample. Samples that satisfy eq 3 fulfill this requirement. The second principle is that the desired chain scattering term must be maximized subject to the first constraint. This is done by choosing the degree of deuteration of the appropriate segment such that the product $x(1 - x)$ is maximized. To satisfy the first principle, it is necessary for there to be some chain scattering from the other segment types in the -HS and -WC samples. For the -HS samples, the chain scattering is due to correlations between the deuterated and protonated hard segments and between the deuterated and protonated soft segments. For the -WC samples, both of the above correlations contribute to the scattering along with the correlations between purely deuterated and protonated chains. The second principle attempts to minimize the contribution from the undesired chain scattering while maximizing the contribution from the desired chain segments.

The final principle arises from the requirement of independence of scattering sites along the polymer chain. For the -HS and -WC samples, two separate polymers must be blended in order to produce the scattering sample. In the case of the -HS samples, a sample has to be prepared with purely deuterated hard segments and one must be made with purely protonated segments in order to get a contrast between the hard segments. These are then blended to form the -HS sample. If the -HS sample is made in one step using a mixture of deuterated and protonated monomers, the resulting hard-segment isotopic distribution would render the sample useless for neutron scattering. The degree of deuteration of each segment type is determined by the second principle, subject to the constraint of the first principle. Similarly, two base materials must be blended together to create the -WC samples.

The values listed in Tables I and II are calculated by using eq 3, the criterion for phase contrast matching, and the mass densities of the crystalline hard segments and the amorphous soft segments. The values used are those reported by Vallance et al.[4] to be 1.403 g/cm^3 for the hard segments and 0.98 g/cm^3 for the soft segments. These values are in close agreement with the densities determined experimentally. The soft-segment density was determined from a measurement of the density of the bulk oligomer. The hard-segment density was determined by measuring the overall sample density and a mass balance. The coherent scattering length densities were calculated by using the values for the atomic and monomeric coherent scattering lengths listed in Table IV.

Table IV
Atomic and Monomer Coherent Scattering Lengths for Common Isotopes

species	$b \times 10^{12}$, cm
H	−0.374
D	0.667
C	0.665
N	0.94
O	0.58
DMT ($C_{10}H_{10}O_2$)	4.07
d-DMT ($C_{10}D_{10}O_2$)	14.48
BD ($C_4H_{10}O_2$)	0.08
d-BD ($C_4D_{10}O_2$)	10.49
THF[a] (C_4H_8O)	0.248
d-THF (C_4D_8O)	8.576
hard-segment repeat unit ($C_{12}H_{12}O_4$)	5.812
d-HS repeat unit ($C_{12}D_{12}O_4$)	18.304
hard-segment end unit ($C_8H_4O_3$)	5.564
d-HS end unit ($C_8D_4O_3$)	9.728

[a] THF (tetrahydrofuran) is the monomer for poly(tetramethylene oxide).

Table V
Radius of Gyration Results for the Polyether Segments for the Random Coil Model

sample	temp, °C	R_g, Å	error,[a] ±Å
5-SS	25	12.8	0.3
	60	12.3	0.3
	95	12.0	0.4
	130	11.5	0.3
	160	11.1	0.3
	190	11.3	0.6
10-SS	25	13.4	0.4
	60	12.9	0.3
	95	13.2	0.4
	130	12.8	0.3
	160	13.1	0.4
	190	12.4	0.3
	210	11.5	0.4

[a] The errors listed are 95% confidence limits determined by the nonlinear regression routine.

Results and Discussion

The results of the model fitting procedure using eq 14 are summarized in Tables V–VII. Table V lists the number-average radius of gyration of the soft segment for samples 5-SS and 10-SS as a function of temperature using the random coil form factor for the chain model. Table VI gives the results for the hard segments in samples 5-HS and 10-HS as a function of temperature for the random coil, cylinder, and rod models. Table VII shows the results for the 5-WC and 10-WC samples for the random coil and cylinder models as a function of temperature. The values given in Tables V–VII have been corrected for the polydispersity of the particular segments according to eq 15b. The data in Table VII have been corrected for polydispersity by assuming that the chain radius of gyration is proportional to the one-half power of the molecular weight and that the size distribution is the most probable for condensation polymers with a degree of completion of the reaction equal to 0.99. Slight mismatches in molecular weight and distribution between the deuterated and protonated chain segments are ignored since these mismatches have little effect on the scattering results.[31]

Table VI
Radius of Gyration Results for the Polyester Segments Using the Random Coil, Cylinder, and Rod Models

sample	temp, °C	R_g, Å	error,[a] ±Å	model type
5-HS	25	12.5	0.6	RC
	60	13.9	0.8	RC
	95	14.6	0.7	RC
	130	15.7	1.0	RC
5-HS	25	12.8	0.6	cyl
	60	12.8	0.7	cyl
	95	14.0	0.7	cyl
	130	15.5	0.7	cyl
5-HS	25	11.4	0.6	rod
	60	12.0	0.7	rod
	95	12.9	0.7	rod
	130	15.1	0.7	rod
10-HS	25	12.8	1.2	RC
	60	15.0	1.4	RC
	95	16.1	1.4	RC
	130	20.1	1.1	RC
	160	24.0	1.3	RC
	190	25.8	4.2	RC
10-HS	25	11.8	1.0	cyl
	60	14.3	1.2	cyl
	95	14.8	1.1	cyl
	130	17.2	0.9	cyl
	160	20.8	1.1	cyl
	190	20.7	3.3	cyl
10-HS	25	11.3	1.0	rod
	60	13.1	1.2	rod
	95	13.7	1.2	rod
	130	18.1	1.1	rod
	160	22.2	1.4	rod
	190	21.9	3.8	rod

[a] Error estimates are 95% confidence limits determined by the nonlinear regression routine.

Table VII
Radius of Gyration Results for the Whole Chain Using the Rod and Cylinder Models

sample	temp, °C	R_g, Å	error,[a] ±Å	model type
5-WC	25	52.6	0.5	RC
	60	50.2	0.5	RC
	95	43.8	0.6	RC
	130	40.9	0.7	RC
	160	37.7	0.5	RC
	190	55.9	1.4	RC
5-WC	25	57.4	0.5	cyl
	60	51.6	0.4	cyl
	95	44.4	0.4	cyl
	130	36.9	0.4	cyl
	160	32.4	0.5	cyl
	190	43.3	0.7	cyl
10-WC	25	67.8	1.0	RC
	60	58.2	1.5	RC
	95	43.5	1.4	RC
	130	34.1	1.2	RC
	160	30.7	1.2	RC
	190	34.3	1.6	RC
	210	51.87	1.1	RC
10-WC	25	75.1	2.0	cyl
	60	69.3	2.0	cyl
	95	69.6	1.0	cyl
	130	34.3	1.1	cyl
	160	24.0	0.5	cyl
	190	26.8	0.6	cyl
	210	40.9	0.5	cyl

[a] Error estimates are 95% confidence limits determined by the nonlinear regression routine.

Figure 3 illustrates the change in the soft-segment chain radius of gyration as a function of temperature for the 5-SS and 10-SS samples. Figure 4 shows a model fit of the random coil model to data for the 10-SS sample at room temperature. The radius of gyration of the soft segment at room temperature is 12.8 Å for the 5-SS sample and 13.4 Å for the 10-SS sample. A value of 12.1 Å is measured by SANS on a bulk oligomeric blend of protonated and deuterated PTMO of 1000 molecular weight.[23] This gives a value of 11.8 Å for a segment with a molecular weight of 950 assuming a value of $^1/_2$ for α. Thus the average soft segment is slightly extended at room temperature. The majority of the soft segments are in a random coil conformation, but a number of them are fairly elongated. As the temperature increases, the soft-segment R_g decreases to 11.1 Å at 160 °C for the 5-SS sample and 11.5 Å at 210 °C for the 10-SS sample, a change of about 15%. The mechanism responsible for this small change in the soft-segment R_g is the relaxation of stresses associated with the elongated segments. These elongated molecules have been termed taut tie molecules.[7,32,33] As the samples are heated above the glass transition temperature of the hard segment, which has been reported to be about 50 °C,[34] the chains can more easily rearrange to a lower energy state, which includes minimizing the strain energy present in the elongated soft-segment chains. The chains that are firmly bound in hard-segment crystallites can only rearrange locally in the amorphous part of the chain. This mechanism is consistent with arguments made by Bandara and Droscher,[32,33] who found that changes in the mechanical properties and the small-angle X-ray scattering behavior of polyether–polyester block copolymers could be brought

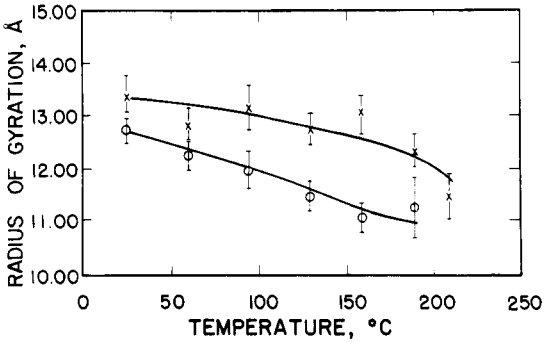

Figure 3. Radius of gyration of the polyether segments in the 5-SS (O) and the 10-SS (×) samples as a function of temperature for the random coil model.

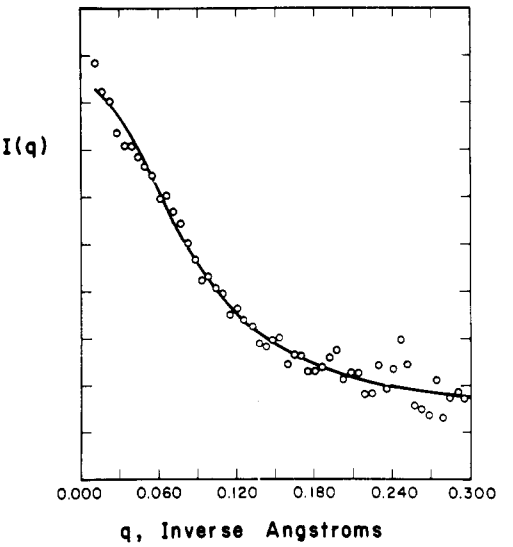

Figure 4. Model fit of the random coil model to the soft-segment single-chain scattering for the 5-SS sample at room temperature.

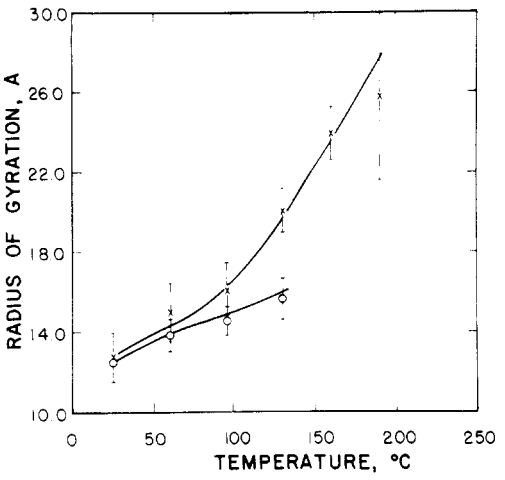

Figure 5. Radius of gyration of the polyester segments in the 5-HS (O) and the 10-HS (×) samples as a function of temperature for the random coil model.

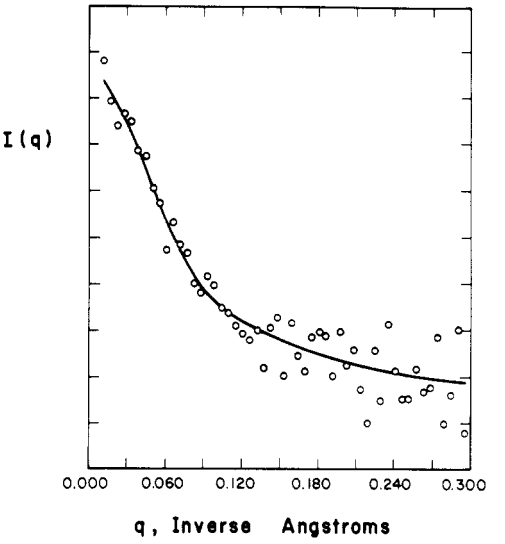

Figure 6. Model fit of the rod model to the single-chain scattering from the polyester hard segments in the 10-HS sample at room temperature.

about by changing the temperature at which the samples are prepared. The loss of mechanical strength with increasing temperature was attributed to a reduction in the number of taut PTMO tie molecules, which is consistent with the reduction of the soft-segment R_g determined in this study. The increase in the SAXS long spacing reported by Bandara and Droscher[32,33] was partially attributed to the decrease in the number of taut tie segments, but the increase is mainly due to changes occuring in the crystalline hard domains.

Figure 5 shows the change in the hard-segment radius of gyration as a function of temperature for the random coil model. The rod and cylinder models give similar results, which are not shown. Figure 6 shows a fit of the cylinder model to the hard-segment single-chain scattering for the 5-HS sample. These data are noisier than the 5-SS data due to the subtraction step used to separate the soft- and hard-segment chain scattering in the original scattering data. The hard-segment radius of gyration increases substantially with increasing temperature. For the 5-HS samples, R_g increases from 12.5 to 15.7 Å, a change of 25%. This compares with a value of 18.0 Å for a hard segment consisting of 5 TMT units in an extended crystal conformation as calculated from data given in a review of poly(tetramethylene terephthalate) crystal structure investigations by Desborough and Hall.[35] The hard-segment R_g in the 10-HS sample increases from 12.8 to 25.8 Å at 190 °C. This compares with a value of 37.6 Å calculated for the extended crystalline conformation of a 10 TMT unit hard segment.

The results of the SANS experiments indicate that chain folding is occurring in the hard segments of these materials. At room temperature, the radius of gyration of the hard segments in both the 5-HS and 10-HS samples is about 12.5 Å. This value is taken from the random coil model results, but the rod and cylinder values are similar, as is the value obtained by using Guinier's law. This is considerably smaller than would be expected if the hard segments were fully extended in the crystal. A fully extended segment that is 3 TMT units long and folds at the oxytetramethylene link would have a radius of gyration about 11.5 Å using an infinitesimal rod approximation. When the width of a folded segment is accounted for, the radius of gyration is expected to be around 11.9 Å for a folded 5 TMT unit hard segment and 12.4 Å for a folded 10 TMT unit hard segment. The close agreement of these figures with the measured values strongly supports the folded-chain model. Van Bogart et al.[36] and Koberstein[37,38] found evidence for chain folding in polyurethane block copolymers. Koberstein states that chain folding must occur in these polyurethanes based on SAXS measurements. The folding length suggested is 3–4 repeat units in the hard segment, which is similar to that suggested by the data in this experiment.

This analysis does not take into account the fact that a substantial number of the hard segments are in the amorphous soft phase. The measured R_g is an average of the crystalline and amorphous conformations. The radius of gyration of the amorphous hard segments is not known, but it must lie between the value for a fully extended chain and a tightly coiled chain. Because of the uncertainty associated with the presence of both amorphous and crystalline hard segments, the folding repeat length cannot be fixed at three TMT units with certainty. Three to four TMT units is a more accurate figure.

When the temperature is increased, the hard-segment radius of gyration also increases. Buck et al.[39,40] reported that the long spacing measured by SAXS in similar materials increased with increasing annealing temperatures. The explanation given for this behavior was that the crystalline hard domain lamellae are thickening. The growth mechanism is similar to that proposed for semicrystalline homopolymers[41] where the thickening process occurs by the extension of folded chains through the melting of the higher energy, multiply folded segments followed by a recrystallization of these melted segments into a more extended, lower energy state. The results of the present investigation support the mechanism of thickening of the lamellar structure through an unfolding of the polyester segments in response to the annealing process. In the 5-HS case, the annealing seems to cause most of the crystallized hard segments to approach the extended crystalline conformation. The difference between the measured radius of gyration and that calculated for an extended chain (15.7 vs. 18.0 Å) can be attributed to the fact that the measured value is an average of the crystalline and amorphous configurations. If one assumes that 50% of the ester sequences are located within the hard phase, the amorphous hard-segment radius of gyration can be calculated to be about 13 Å. The 10-HS hard segments unfold to a greater extent than do those of the 5-HS sample because the 10-HS hard segments start out with a greater amount of chain folding. When the presence of

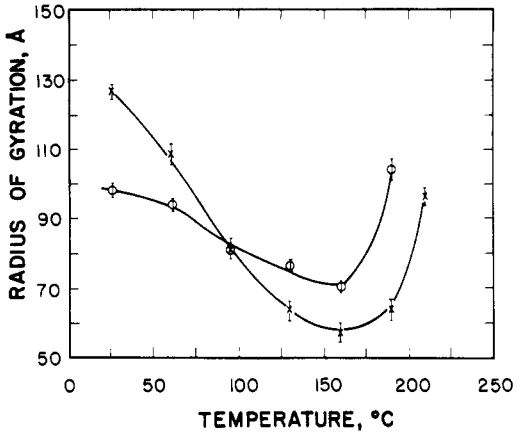

Figure 7. Radius of gyration of the total polymer chain as a function of temperature for samples 5-WC (O) and 10-WC (×) using the random coil model.

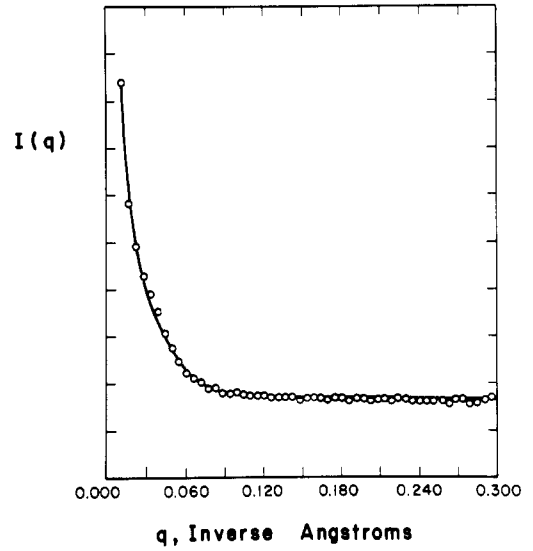

Figure 8. Model fit for the cylindrical model to the single-chain scattering data from the entire polyether–polyester chain for the 5-WC sample at room temperature.

amorphous hard segments in the soft phase is accounted for, it can be concluded that there still is some chain folding in the 10-HS samples at elevated temperatures. Many of the hard segments are too long to reach an extended state.

The overall chain radius of gyration is shown as function of temperature in Figure 7. Figure 8 shows the fit of the cylinder model to the 10-WC whole-chain scattering data. The whole-chain R_g is seen to decrease with increasing temperature up to 150 °C. Above this temperature, an upturn is observed in R_g. The reason for this is unclear. One possible explanation is that as the temperature rises, the increase in the chain mobility facilitates the relaxation of stresses frozen into the system by the process of molding the scattering samples below the hard-segment crystalline melting temperature and quickly cooling the sample to room temperature. As the temperature rises, another process also occurs, the growth of the lamellae. This growth occurs mostly in the lateral direction due to accumulation of new hard segments from the soft phase[39,40] but also proceeds by a thickening of the lamellae due to the unfolding of the hard segments at the elevated temperatures. At lower temperatures, the first process dominates and the whole-chain R_g decreases. At higher temperatures, when the rate of crystalline lamellar growth is higher and most of the initial internal stresses have been annealed out, the whole-chain R_g increases.

Conclusions

The conformations of the polyether soft segment, the polyester hard segment, and the entire chain have been measured as a function of temperature for a set of polyether–polyester block copolymers using small-angle neutron scattering. The samples used were prepared so that the coherent scattering length densities of the soft amorphous phase and the crystalline hard phase were identical. This condition, called the phase contrast matched criterion, causes the interphase scattering as well as the interchain scattering between different segment types to vanish, leaving only intrachain and incoherent scattering. The single-chain scattering functions obtained were modeled by using an interactive nonlinear regression analysis for several particle shapes: a random coil, a cylinder, and an infinitesimally thin rod.

The soft-segment R_g was found to decrease as the temperature was increased. The magnitude of the decrease was about 15%. The conformation goes from a slightly elongated random coil to a random coil conformation. This is caused by a relaxation of initial stresses present in the system due to an increase in chain mobility at higher temperatures. The mechanism involves a reduction in the number of taut tie molecules as temperature is increased.[32,33]

The polyester hard segments are chain folded in the crystalline form at room temperature. The evidence for this is twofold. First, the hard-segment R_g changes very little when the average length is increased from 5 to 10 TMT units. Second, the agreement between the experimentally determined R_g and that calculated from an extended crystal structure containing three TMT units is excellent. This repeat length is similar to the proposed repeat length in the hard segments of polyurethane elastomers.[36–38]

As the temperature is increased, the hard-segment chains attain a larger radius of gyration. In the 5-HS sample, many of the crystalline segments become fully extended. The calculated R_g of 18.0 Å for an extended conformation agrees well with the measured value of 15.7 Å when one considers that the measured value is an average of the crystalline and amorphous hard segments. At higher temperatures, the 10-HS hard segments show a larger radius of gyration than the 5-HS hard segments, but fewer 10-HS segments become fully extended. Some chain folding is still present. The mechanism responsible for the unfolding of the hard segments is the melting and recrystallization of higher energy, tightly folded segments into a lower energy, more fully extended state. The morphological change caused by the unfolding of the hard chains is a thickening of the crystalline lamellae. This is supported by small-angle X-ray scattering investigations of the spacing between domains.[32,33,39,40]

The overall chain conformation is also affected by an increase in temperature. Between room temperature and 150 °C, a decrease is seen in the whole-chain radius of gyration. While the exact mechanism is unknown, it may be due to a relaxation of stresses frozen in the material by the initial process of molding below the crystalline melting temperature of the hard segments followed by a rapid cooling of the sample. As the temperature increases above 150 °C, the rate of crystallization of new hard-segment material increases rapidly and becomes the dominant process in the system. As the lamellae get larger, stresses are again applied to the chains, with the result that the radius of gyration increases.

Acknowledgment. J.A.M. and S.L.C. acknowledge partial support of this research by the Polymer Section of the Division of Materials Research of the National Science Foundation under Grant No. DMR 81-06888.

References and Notes

(1) C. K. Shih and J. M. McKenna, *Rubber Chem. Technol.*, to be published.
(2) A. Lilaonitkul and S. L. Cooper, *Macromolecules*, **12**, 1146 (1979).
(3) A. Lilaonitkul and S. L. Cooper, *Rubber Chem. Technol.* **50**, 1 (1977).
(4) M. A. Vallance and S. L. Cooper, *Macromolecules*, **17**, 1208 (1984).
(5) J. W. C. Van Bogart, P. E. Gibson, and S. L. Cooper, *Rubber Chem. Technol.*, **54**, 963 (1981).
(6) G. Perego, M. Cesari, and R. Vitali, *J. Appl. Polym. Sci.*, **29**, 1141 (1984).
(7) G. Perego, M. Cesari, and R. Vitali, *J. Appl. Polym. Sci.*, **29**, 1157 (1984).
(8) J. W. C. Van Bogart, A. Lilaonitkul, L. E. Lerner, and S. L. Cooper, *J. Macromol. Sci., Phys.*, **17**, 267 (1980).
(9) U. Bandara and M. Droscher, *Colloid Polym. Sci.*, **261**, 26 (1983).
(10) F. G. Schmidt and M. Droscher, *Makromol. Chem.*, **184**, 2669 (1983).
(11) J. A. Miller, S. B. Lin, K. K. S. Hwang, K. S. Wu, P. E. Gibson, and S. L. Cooper, *Macromolecules*, **18**, 32 (1985).
(12) D. G. H. Ballard, G. D. Wignall, and J. Schelten, *Eur. Polym. J.*, **9**, 965 (1973).
(13) P. J. Flory, "Principles of Polymer Chemistry", Cornell University Press, Ithaca, NY, 1951.
(14) J. S. Higgins and R. S. Stein, *J. Appl. Crystallogr.*, **11**, 346 (1978).
(15) R. W. Richards, in "Developments in Polymer Characterization", Applied Science Publishers, London (1978).
(16) G. Hadziioannou, C. Picot, A. Skoulios, M. L. Ionescu, A. Mathis, R. Duplessix, Y. Gallot, and J. P. Lingelser, *Macromolecules*, **15**, 263 (1982).
(17) J. T. Koberstein, *J. Polym. Sci., Polym. Phys. Ed.*, **20**, 593 (1982).
(18) S. N. Jahshan and G. C. Summerfield, *J. Polym. Sci., Polym. Phys. Ed.*, **18**, 1859 (1980).
(19) S. N. Jahshan and G. C. Summerfield, *J. Polym. Sci., Polym. Phys. Ed.*, **18**, 2145 (1980).
(20) F. S. Bates, C. V. Berney, R. E. Cohen, and G. D. Wignall, *Polymer*, **25**, 519 (1983).
(21) J. A. Miller, S. L. Cooper, C. C. Han, and G. Pruckmayr, *Macromolecules*, **17**, 1063 (1984).
(22) W. K. Witsiepe, *Adv. Chem. Ser.*, **No. 129**, 39 (1973).
(23) J. A. Miller and S. L. Cooper, *Makromol. Chem.*, **185**, 2429 (1984).
(24) "IPNS Progress Report 1981-1983", Argonne National Laboratory, Argonne, IL, Oct 1983.
(25) A. Z. Akcasu, G. C. Summerfield, S. N. Jahshan, C. C. Han, C. U. Kim, and H. Yu, *J. Polym. Sci., Polym. Phys. Ed.*, **18**, 865 (1980).
(26) G. D. Wignall, R. W. Hendricks, W. C. Koehler, J. S. Lin, M. P. Wai, E. L. Thomas, and R. S. Stein, *Polymer*, **22**, 886 (1981).
(27) L. H. Peebles, *Macromolecules*, **7**, 872 (1974).
(28) L. H. Peebles, *Macromolecules*, **9**, 58 (1976).
(29) G. Hadziioannou, J. Gilmer, and R. S. Stein, *Polym. Bull.*, **9**, 563 (1983).
(30) A. Guinier and G. Fournet, "Small-Angle Scattering of X-Rays", Wiley, New York, 1955.
(31) C. Tangari, J. S. King, and G. C. Summerfield, *Macromolecules*, **15**, 132 (1982).
(32) U. Bandara and M. Droscher, *Angew. Makromol. Chem.*, **107**, 1 (1982).
(33) M. Droscher, *Adv. Polym. Sci.*, **47**, 119 (1982).
(34) W. Marrs, R. H. Peters, and R. H. Still, *J. Appl. Polym. Sci.*, **23**, 1063 (1979).
(35) I. J. Desborough and I. H. Hall, *Polymer*, **18**, 825 (1977).
(36) J. W. C. Van Bogart, P. E. Gibson, and S. L. Cooper, *J. Polym. Sci., Polym. Phys. Ed.*, **21**, 65 (1983).
(37) J. T. Koberstein and R. S. Stein, *J. Polym. Sci., Polym. Phys. Ed.*, **21**, 1439 (1983).
(38) L. M. Leung and J. T. Koberstein, *J. Polym. Sci., Polym. Phys. Ed.*, submitted for publication.
(39) W. H. Buck, R. J. *Cella*, E. K. Gladding, and J. R. Wolfe, *J. Polym. Sci., Polym. Symp.*, **No. 48**, 47 (1974).
(40) W. H. Buck and R. J. Cella, *Polym. Prepr., Am. Chem. Soc., Div. Polym. Chem.*, **14**, 98 (1973).
(41) A. Keller, *Rep. Prog. Phys.*, **31**, 623 (1968).
(42) A. Maconnachie, *Polymer*, **25**, 1068 (1984).
(43) D. G. H. Ballard, M. G. Rayner, and J. Schelten, *Polymer*, **17**, 349 (1976).

Light Scattering Study of Three-Component Systems. 1. Excluded Volume Effect of Poly(methyl methacrylate) in the Binary Mixture 1-Chlorobutane + 2-Methoxyethanol

Mitsuo Nakata* and Naoko Numasawa†

Department of Polymer Science, Faculty of Science, Hokkaido University, Sapporo, Japan.
Received November 26, 1984

ABSTRACT: Light scattering measurements have been made on dilute solutions of poly(methyl methacrylate) ($M_w = 2.44 \times 10^6$) in the mixed solvent 1-chlorobutane (BuCl) + 2-methoxyethanol (MOEt) at 40 °C. On account of a very small refractive index difference between BuCl and MOEt, the light scattering data were analyzed as in the case of polymer solutions of a single solvent to determine the molecular weight M_w, the mean-square radius of gyration $\langle s^2 \rangle$, and the second virial coefficient A_2. The molecular weight obtained from zero-angle scattering was independent of the composition of the mixed solvent. A_2 and $\langle s^2 \rangle$, obtained as a function of the volume fraction u_2 of MOEt in the mixed solvent, showed a large maximum value at the same u_2. The behavior of the universal function Ψ as a function of the expansion factor α showed the same trend as those observed in experiments with a single solvent. In the framework of the two-parameter theory, the excluded volume effect in the present ternary system did not show a clear difference from that in systems of a single solvent. From the magnitude of the excluded volume of the polymer segment, the mixed solvent was found to act as a good solvent for poly(methyl methacrylate).

I. Introduction

Dilute polymer solutions in mixed solvents show different behavior from those in the constituent single solvents. The second virial coefficient A_2 and the intrinsic viscosity $[\eta]$ in mixed solvents have been found to be larger than those in the constituent single solvents.[1-6] Even nonsolvents for a polymer can become good solvents for the polymer when mixed.[5-8] The behaviors of dilute polymer solutions in a mixed solvent and in its constituent single solvents have been compared by evaluating excluded

†Present address: Department of Polymer Chemistry, Tokyo Institute of Technology, Ookayama, Meguro-ku, Tokyo 152, Japan.

0024-9297/85/2218-1736$01.50/0